Journal of Japan Association for Earthquake Engineering, Vol. 25, No. 13, 2025
[Technical Paper (Translated Paper)]

EIGENVALUE PROBLEM OF MDOF NON-PROPORTIONAL COMPLEX DAMPING SYSTEM AND TRANSFER FUNCTION BY MODE SUPERPOSITION

Yuzuru YASUI[1], Toshiro MAEDA[2] and Michio IGUCHI[3]

[1] Member, Dr. Eng., Adjunct Researcher, Research Institute for Science and Engineering, Waseda University,
Tokyo, Japan, yasui@mx5.mesh.ne.jp
[2] Member, Dr. Eng., Professor, Department of Architecture, School of Creative Science and Engineering, Waseda University,
Tokyo, Japan, tmaeda@waseda.jp
[3] Member, Dr. Eng., Emeritus Professor, Tokyo University of Science,
Tokyo, Japan, iguchi@rs.noda.tus.ac.jp

ABSTRACT: First, we present a method for obtaining the eigenvalues and eigenvectors of a multi-degree-of-freedom system with nonproportional complex damping. These eigenvalues and eigenvectors are complex and appear in conjugate pairs, corresponding to the number of masses, with forward waves and their conjugate backward waves. By leveraging the orthogonality of the eigenvectors, we show that the seismic transfer function for each mass can be expressed as a superposition of the transfer functions of the complex modes of the forward wave, exhibiting conjugate symmetry. Similarly, using the orthogonality of the real eigenvectors, we derive an approximate transfer function by superimposing the transfer functions of the real modes. Finally, numerical calculations using a simple model are performed to validate the proposed complex eigenvalue analysis method and the transfer function based on complex modes. Additionally, we discuss the reliability of the transfer function derived from real modes.

Keywords: *Multi-degree-of-freedom system, Complex damping, Nonproportional damping, Complex eigenvalue analysis, Transfer function, Mode superposition method*

1. INTRODUCTION

It has been suggested that the damping of structures may be complex damping (also referred to as hysteresis damping or structural damping), which remains constant[1), 2)] with respect to frequency, rather than viscous damping, which is proportional to frequency. The concept of complex damping was originally introduced in the harmonic vibration analysis of aircraft flutter[3)] and has since been incorporated into the equations of motion of structures[4)]. Its application has raised several issues, mainly in the context of single-degree-of-freedom (SDOF) systems, as summarized below:

(1) Differences from the viscous damping case in parameters such as the damped natural frequency[4].
(2) The inconsistency between equations of motion in the frequency domain and those in the time domain[5, 6].
(3) The necessity of introducing the sign function to ensure that the response remains a real value[6].
(4) The issue that the impulse response, obtained via the inverse Fourier transform of the transfer function, becomes non-causal[6], and the challenges associated with evaluating the integral of the inverse Fourier transform[7, 8].
(5) The proposal of an equivalent viscous damping model[6].

Among these issues, if we accept that the response is non-causal, the remaining major concern is the second issue, i.e., the inconsistency between equations of motion in different domains, for which a solution has been sought.

Inaudi and Kelly[9] proposed a time-domain representation of the equation of motion, incorporating the damping force as the product of the imaginary part of the complex stiffness and the Hilbert transform of the displacement response. The Fourier transform of this equation of motion is consistent with the well-known frequency-domain equation, thereby resolving the above inconsistency. Building upon this approach, the authors[10] demonstrated that the complex eigenvalues of the forward and backward waves for an SDOF system can be obtained. In doing so, they noted that the displacement response in free vibration consists of a single frequency component and that the Hilbert transform of a free wave is equivalent to advancing the phase by $\pi/2$[11, 12].

In recent years, the number of buildings employing base-isolation and vibration control systems has been increasing. To evaluate the seismic damping effectiveness of such structures, it would be beneficial to develop a method for complex eigenvalue analysis of multi-degree-of-freedom (MDOF) systems with nonproportional complex damping, where damping values vary across different parts of the system. Additionally, a modal analysis method utilizing these results would be useful. Although pioneering studies[13, 14] have explored this approach, their theoretical formulations remain incomplete. Therefore, there is a need to establish a theoretically consistent method for complex eigenvalue analysis of MDOF systems with nonproportional complex damping.

In this paper, we first present a method for obtaining the complex eigenvalues and complex eigenvectors of the forward and backward waves in an MDOF system by solving the eigenvalue problem for the time-domain equation of motion, including the damping force proposed by Inaudi and Kelly. When applying Hilbert transform, we note that, as in the SDOF case, free vibration consists of a single frequency component. Utilizing the orthogonality of the complex eigenvectors, we show that the transfer function of each mass can be obtained by superimposing the transfer functions of the complex modes. Since these transfer functions exhibit conjugate symmetry, only the complex eigenvalues and eigenvectors of the forward waves (equal in number to the masses) are required for calculations. This makes the method significantly more efficient than the nonproportional viscous damping approach[15], which requires twice as many eigenvalues and mode shapes as the number of masses. Next, as an approximate method, we show that the transfer function of each mass can be obtained by superimposing the transfer functions of real modes, derived from real eigenvalue analysis. Seismic response calculations are performed using a modal analysis approach, which involves superimposing the responses obtained via the inverse Fourier transform[16] of the product of the Fourier transform of the input acceleration and the transfer function of each mode. The following sections describe the complex eigenvalue analysis method and the derivation of transfer functions, followed by numerical simulations using a vibration control structure[17] as an example to validate the complex modal approach and assess the applicability of the real modal approach. It should be noted that the response prediction method proposed in this study is based on the assumption of linear response.

2. EQUATION OF MOTION AND TRANSFER FUNCTION

Consider the case where the ground acceleration $\ddot{x}_g$ is applied to the base of the shear-type n-mass

model shown in Fig. 1. Let m_i be the i-th mass of this system and let k_i and k_i' be the real and imaginary parts of the complex stiffness of the i-th story, respectively. Also, let x_i be the displacement of the i-th mass relative to the base. The time-domain equation of motion, following Inaudi and Kelly[9], is given by

$$[M]\{\ddot{x}\} + [K]\{x\} + [K']\{\hat{x}\} = -[M]\{1\}\ddot{x}_g \tag{1}$$

where $[M]$: mass matrix, $[K]$: matrix consisting of the real part of complex stiffness, $[K']$: matrix consisting of the imaginary part of the complex stiffness and, $\{x\}$: displacement vector with x_i as its elements, $\{1\}$: n-dimensional vector with all elements equal to 1, x_g: ground displacement, $\ddot{A}$: second-order derivative of A with respect to time t. Additionally, $\{\hat{x}\}$ is a vector whose elements are the Hilbert transform $\hat{x}_i$ of x_i, given by

$$\hat{x}_i(t) = \int_{-\infty}^{\infty} \frac{-x_i(\tau)}{\pi(t-\tau)}\, d\tau \tag{2}$$

When $[K']$ is proportional to $[K]$, the system exhibits proportional damping; otherwise, it is classified as nonproportional damping. The damping ratio h_i for the ith story is defined as

$$h_i = \frac{1}{2}\frac{k_i'}{k_i} \tag{3}$$

In the case of proportional damping, h_i takes the same value for each layer.

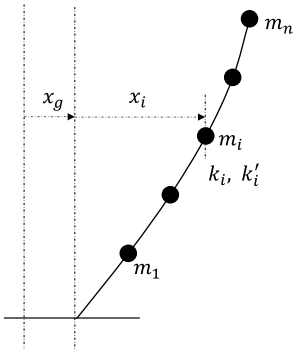

Fig. 1 Lumped mass model

Applying the Fourier transform to Eq. (1) yields

$$-\omega^2[M]\{X(j\omega)\} + ([K] + j[K']\,\mathrm{sgn}(\omega))\{X(j\omega)\} = -[M]\{1\}X_g(j\omega) \tag{4}$$

where, $\{X(j\omega)\}$: a vector whose elements are $X_i(j\omega)$, the Fourier transform of $x_i(t)$, $X_g(j\omega)$: the Fourier transform of $\ddot{x}_g(t)$, j : imaginary unit, ω : circular frequency, and $A(j\omega)$: a complex function of ω.

In deriving Eq. (4), the Fourier transform of $\hat{x}_i(t)$ is given by

$$\mathrm{FT}[\hat{x}_i(t)] = j\,\mathrm{sgn}(\omega)\, X_i(j\omega) \tag{5}$$

where $\mathrm{sgn}(\omega)$ is the sign function, defined as

$$\mathrm{sgn}(\omega) = 1\ (\omega > 0),\ \ 0\ (\omega = 0),\ \ -1(\omega < 0) \tag{6}$$

From Eqs. (1) and (4), it is confirmed that the equations of motion in the time and frequency domains are consistent, thereby resolving the inconsistency issue previously reported[5), 6)]. Eq. (6) also indicates that Eq. (4) must be treated separately for the cases of forward waves ($\omega > 0$), stationary state ($\omega = 0$), and backward waves ($\omega < 0$). Furthermore, Eq. (5) shows that the Hilbert transform shifts the phase of all frequency components by $\pi/2$[11), 12)]. Therefore, when the frequency is known, Eq. (5) provides a more convenient representation than Eq. (2).

From Eq. (4), solving for $\{X(j\omega)\}$ and taking its ratio to $X_g(j\omega)$, we obtain the transfer function $\{G_d^o(j\omega)\}$ for the relative displacement:

$$\{G_d^o(j\omega)\} = -(-\omega^2[M] + [K] + j[K']\,\mathrm{sgn}(\omega))^{-1}[M]\{1\} \tag{7}$$

where $\{G_d^o(j\omega)\}$ is a column vector whose elements are the transfer functions $G_{d,i}^o(j\omega)$ for each mass. From Eq. (7), it follows that $\{G_d^o(-j\omega)\}$ is equal to conjugate of $\{G_d^o(j\omega)\}$, confirming that the relation is conjugate symmetric.

The transfer functions for relative velocity $\{G_v^o(j\omega)\}$ and absolute acceleration $\{G_a^o(j\omega)\}$ can be obtained using $\{G_d^o(j\omega)\}$ as follows:

$$\{G_v^o(j\omega)\} = j\omega\{G_d^o(j\omega)\},\quad \{G_a^o(j\omega)\} = 1 - \omega^2\{G_d^o(j\omega)\} \tag{8a,b}$$

For brevity, the remainder of this paper will focus on the transfer function for relative displacement.

The seismic response is obtained by applying the inverse Fourier transform[16)] to the product of the transfer function (Eq. (7) or Eq. (8)) and the Fourier transform of the input motion. To predict or interpret the results, it is useful to analyze the natural frequencies, damping constants, and stimulus functions of each mode.

3. EIGENVALUE ANALYSIS

3.1 Eigenvalue problem

Setting the right-hand side of Eq. (1) to zero yields the homogeneous equation:

$$[M]\{\dot{x}\} + [K]\{x\} + [K']\{\hat{x}\} = 0 \tag{9}$$

Now, let the solution of Eq. (9) be expressed as

$$\{x\} = \{u^*\}e^{j\omega^* t} \tag{10}$$

In Eq. (10), $\{u^*\}$ is a complex column vector, and ω^* is the complex circular frequency. The notation A^* indicates that A is a complex quantity.

Substituting Eq. (10) into Eq. (9) and dividing both sides by $e^{j\omega^* t}$ yields

$$\left(-\omega^{*2}[M] + [K] + j[K']\,\mathrm{sgn}(\mathrm{Re}\,\omega^*)\right)\{u^*\} = \{0\} \tag{11}$$

Here, in the derivation of Eq. (11), the Hilbert transform of $e^{j\omega^* t}$, denoted as $H\left[e^{j\omega^* t}\right]$, is assumed to be

$$H\left[e^{j\omega^* t}\right] = je^{j\omega^* t}\,\mathrm{sgn}(\mathrm{Re}\,\omega^*) \tag{12}$$

Equation (12) is derived by shifting the phase of $e^{j\mathrm{Re}\,\omega^* t}$ by $\pi/2$[11), 12)], without using Eq. (2), since the free vibration solution consists of a single circular frequency component, $\mathrm{Re}\,\omega^*$. Note that $e^{-\mathrm{Im}\,\omega^* t}$ is not affected by the Hilbert transform because it has no phase information.

Equation (11) represents an eigenvalue problem for determining the eigenvalues ${\omega^*}^2$ and eigenvectors $\{u^*\}$. However, it is necessary to separately consider the cases of forward waves $\mathrm{Re}\,\omega^* > 0$ and backward waves $\mathrm{Re}\,\omega^* < 0$.

3.2 Eigenvalues and orthogonality for forward waves

First, consider the case where $\mathrm{Re}\,\omega^* > 0$. In this case, Eq. (11) simplifies to

$$\left(-{\omega^*}^2[M] + [K] + j[K']\right)\{u^*\} = \{0\} \tag{13}$$

Solving Eq. (13) yields n eigenvalues ${}_s{\omega^*}^2 (s = 1\sim n)$ and corresponding eigenvectors $\{{}_s u^*\} (s = 1\sim n)$. A brief examination shows that these eigenvectors satisfy the orthogonality conditions:

$$\{{}_r u^*\}^T[M]\{{}_s u^*\} = \{0\} \quad (r \neq s), \quad \{{}_r u^*\}^T([K] + j[K'])\{{}_s u^*\} = \{0\} \quad (r \neq s) \tag{14a, b}$$

Using Eq. (14a), any vector $\{w\}$ can be expanded as a linear combination of the n eigenvectors:

$$\{w\} = \sum_{s=1}^{n} {}_s\alpha^* \{{}_s u^*\}, \quad {}_s\alpha^* = \frac{\{{}_s u^*\}^T[M]\{w\}}{\{{}_s u^*\}^T[M]\{{}_s u^*\}} \tag{15a, b}$$

3.3 Complex eigenvalues and damping

The eigenvalues of the s-th mode, ${}_s{\omega^*}^2$, can be expressed as

$${}_s{\omega^*}^2 = {}_s\omega^2(1 + j2\,{}_s h), \quad {}_s\omega^2 = \mathrm{Re}\,{}_s{\omega^*}^2, \quad {}_s h = \frac{1}{2}\frac{\mathrm{Im}\,{}_s{\omega^*}^2}{\mathrm{Re}\,{}_s{\omega^*}^2} \tag{16a, b, c}$$

here, ${}_s\omega$ and ${}_s h$ represent the undamped natural circular frequency and complex damping constant for the s-th mode, respectively. Of the two solutions obtained from Eq. (16a), the one satisfying $\mathrm{Re}\,\omega^* > 0$ corresponds to the desired natural frequency ${}_s\omega_1^*$, given by[10)]

$${}_s\omega_1^* = \sqrt{1 + {}_s h_e{}^2}\,{}_s\omega + j\,{}_s h_e\,{}_s\omega, \quad {}_s h_e = \sqrt{\frac{\sqrt{1 + 4\,{}_s h^2} - 1}{2}} \tag{17a, b}$$

The parameter ${}_s h_e$ in Eq. (17b) represents the damping effect and is approximately equal to ${}_s h$ (e.g., when ${}_s h = 0.2$, then ${}_s h_e \approx 0.196$). The real part of Eq. (17a) corresponds to the damped natural frequency, which increases with damping, while the imaginary part represents the exponential decay. These quantities are fully determined once ${}_s\omega$ and ${}_s h$ are known. The derivation of Eq. (17) from Eq. (16a) is detailed in Appendix-1.

3.4 Backward waves and conjugate eigenvalues

Since the eigenvalues ${}_s{\omega^*}^2$ and eigenvectors $\{{}_s u^*\}$ satisfy Eq. (13), we obtain

$$\left(-{}_s{\omega^*}^2[M] + [K] + j[K']\right)\{{}_s u^*\} = \{0\} \tag{18}$$

Taking the complex conjugate of both sides of Eq. (18) gives

$$\left(-{}_s\bar{\omega}^{*2}[M]+[K]-j[K']\right)\{{}_s\bar{u}^*\}=\{0\} \tag{19}$$

where $\bar{A}^*$ denotes the conjugate of A^*. This result confirms that for $\mathrm{Re}\,\omega^*<0$, the eigenvalues are ${}_s\bar{\omega}^{*2}$, and the corresponding eigenvectors are $\{{}_s\bar{u}^*\}$.

From Eq. (16a), ${}_s\bar{\omega}^{*2}$ is given by

$${}_s\bar{\omega}^{*2}={}_s\omega^2(1-j2{}_sh) \tag{20}$$

Among the two roots of Eq. (20), the one satisfying $\mathrm{Re}\,{}_s\bar{\omega}^*<0$ is the desired complex natural circular frequency. This is denoted again as ${}_s\omega_2^*$, and can be written as[10)]

$${}_s\omega_2^*=-\sqrt{1+{}_sh_e{}^2}\,{}_s\omega+j{}_sh_e{}_s\omega \tag{21}$$

Furthermore, for the conjugate eigenvectors $\{{}_s\bar{u}^*\}$, the following orthogonality conditions hold:

$$\{{}_r\bar{u}^*\}^T[M]\{{}_s\bar{u}^*\}=\{0\}\quad(r\neq s),\qquad \{{}_r\bar{u}^*\}^T([K]-j[K'])\{{}_s\bar{u}^*\}=\{0\}\quad(r\neq s) \tag{22a,b}$$

Using Eq. (22a), any vector $\{w\}$ can also be expressed as a linear combination of the conjugate eigenvectors:

$$\{w\}=\sum_{s=1}^{n}{}_s\bar{\alpha}^*\{{}_s\bar{u}^*\},\qquad {}_s\bar{\alpha}^*=\frac{\{{}_s\bar{u}^*\}^T[M]\{w\}}{\{{}_s\bar{u}^*\}^T[M]\{{}_s\bar{u}^*\}} \tag{23a,b}$$

3.5 Generalized complex mass and stiffness

Now, multiplying Eq. (18) for $\mathrm{Re}\,\omega^*>0$ by $\{{}_su^*\}^T$ and considering Eq. (16a), we obtain

$${}_s\omega^{*2}=\frac{{}_sK^*+j{}_sK'^*}{{}_sM^*}={}_s\omega^2(1+j2{}_sh) \tag{24}$$

where ${}_sM^*$: generalized complex mass for the s-th mode, ${}_sK^*$: generalized real stiffness for the s-th mode, ${}_sK'^*$: generalized image stiffness for the s-th mode, and these are defined as follows:

$${}_sM^*=\{{}_su^*\}^T[M]\{{}_su^*\},\quad {}_sK^*=\{{}_su^*\}^T[K]\{{}_su^*\},\quad {}_sK'^*=\{{}_su^*\}^T[K']\{{}_su^*\} \tag{25a,b,c}$$

Similarly, multiplying Eq. (19) for $\mathrm{Re}\,\omega^*<0$ by $\{{}_s\bar{u}^*\}^T$ and considering Eq. (20), we obtain

$${}_s\bar{\omega}^{*2}=\frac{{}_s\bar{K}^*-j{}_s\bar{K}'^*}{{}_s\bar{M}^*}={}_s\omega^2(1-j2{}_sh) \tag{26}$$

where

$${}_s\bar{M}^*=\{{}_s\bar{u}^*\}^T[M]\{{}_s\bar{u}^*\},\qquad {}_s\bar{K}^*=\{{}_s\bar{u}^*\}^T[K]\{{}_s\bar{u}^*\},\quad {}_s\bar{K}'^*=\{{}_s\bar{u}^*\}^T[K']\{{}_s\bar{u}^*\} \tag{27a,b,c}$$

4. TRANSFER FUNCTION BASED ON COMPLEX EIGENMODES

In Eq. (4), we consider the case where $\omega > 0$ and divide the displacement solution $\{X(j\omega)\}$ by $X_g(j\omega)$ to obtain the transfer function $\{G_d(j\omega)\}$, which is expressed as a superposition of complex eigenmodes $\{{}_s u^*\}$. That is,

$$\{G_d(j\omega)\} = \sum_{s=1}^{n} {}_s\beta^* \{{}_s u^*\} \, {}_s q_d(j\omega) \tag{28}$$

where ${}_s q_d(j\omega)$ is a function of frequency representing the contribution of the s-th mode, and ${}_s\beta^*$ is the complex stimulus coefficient. This is equal to the coefficient obtained when the vector $\{1\}$ is expanded in Eq. (15), namely:

$$\{1\} = \sum_{s=1}^{n} {}_s\beta^* \{{}_s u^*\}, \quad {}_s\beta^* = \frac{\{{}_s u^*\}^T [M] \{1\}}{\{{}_s u^*\}^T [M] \{{}_s u^*\}} \tag{29a,b}$$

Note that ${}_s\beta^* \{{}_s u^*\}$ is called the complex stimulus function, and its sum equals $\{1\}$, as shown in Eq. (29a).

Substituting $\{X(j\omega)\} = X_g(j\omega)\{G_d(ji\omega)\}$ and Eq. (29a) into Eq. (4) for ω > 0, then multiplying by $\{{}_s u^*\}^T$ and considering the orthogonality in Eq. (14), we obtain:

$${}_s q_d(j\omega) = -\frac{1}{-\omega^2 + \frac{{}_s K^* + j\,{}_s K'^*}{{}_s M^*}} \tag{30}$$

Now, by replacing the second term in the denominator of Eq. (30) with Eq. (24), we obtain Eq. (31) using ${}_s\omega$ and ${}_s h$ as follows:

$${}_s q_d(j\omega) = -\frac{1}{{}_s\omega^2} \frac{1}{1 - \left(\frac{\omega}{{}_s\omega}\right)^2 + j2\,{}_s h} \tag{31}$$

Next, considering $\omega < 0$ in Eq. (4) and expressing the ratio of the solution $\{X(j\omega)\}$ to $X_g(j\omega)$ as a superposition of eigenmodes $\{{}_s \bar{u}^*\}$, and applying the same procedure, we obtain the transfer function $\{\bar{G}_d(j\omega)\}$, which exhibits conjugate symmetry with $\{G_d(j\omega)\}$, as follows:

$$\{\bar{G}_d(j\omega)\} = \sum_{s=1}^{n} {}_s\bar{\beta}^* \{{}_s \bar{u}^*\} \, {}_s \bar{q}_d(j\omega) \tag{32}$$

where:

$$\{1\} = \sum_{s=1}^{n} {}_s\bar{\beta}^* \{{}_s \bar{u}^*\}, \quad {}_s\bar{\beta}^* = \frac{\{{}_s \bar{u}^*\}^T [M] \{1\}}{\{{}_s \bar{u}^*\}^T [M] \{{}_s \bar{u}^*\}} \tag{33a,b}$$

and:

$${}_s \bar{q}_d(j\omega) = -\frac{1}{{}_s\omega^2} \frac{1}{1 - \left(\frac{\omega}{{}_s\omega}\right)^2 - j2\,{}_s h} \tag{34}$$

At the singular point, $\omega = 0$ ($\mathrm{sgn}(\omega) = 0$), the transfer function is given by the following

equation when the s-th eigen circular frequency of the real eigenvalue problem is ${}_s\omega_0$ and the corresponding eigenvector is $\{{}_su\}$:

$$\{G_d(0)\} = -\sum_{s=1}^{n} {}_s\beta\{{}_su\}\frac{1}{{}_s\omega_0^2} \tag{35}$$

where:

$$\{1\} = \sum_{s=1}^{n} {}_s\beta\{{}_su\}, \quad {}_s\beta = \frac{\{{}_su\}^T[M]\{1\}}{\{{}_su\}^T[M]\{{}_su\}} \tag{36a,b}$$

here, ${}_s\beta$ is the real stimulus coefficient, and ${}_s\beta\{{}_su\}$ is the real stimulus function.

5. TRANSFER FUNCTION BASED ON REAL MODES

In Eq. (4), we consider the case $\omega > 0$ and divide the displacement solution $\{X(j\omega)\}$ by $X_g(j\omega)$ to obtain $\{G_{0d}(j\omega)\}$, which is expressed as a superposition of real eigenmodes $\{{}_su\}$. In other words:

$$\{G_{0d}(j\omega)\} = \sum_{s=1}^{n} {}_s\beta\{{}_su\}\,{}_sq_{0d}(j\omega) \tag{37}$$

Substituting $\{X(j\omega)\} = X_g(j\omega)\{G_{0d}(j\omega)\}$ and Eq. (36a) into Eq. (4) for $\omega > 0$, multiplying by $\{{}_su\}^T$, considering the orthogonality conditions given in Eq. (38a) and (38b), as well as the approximate orthogonality condition given in Eq. (38c):

$$\{{}_ru\}^T[M]\{{}_su\} = 0, \quad \{{}_ru\}^T[K]\{{}_su\} = 0, \quad \{{}_ru\}^T[K']\{{}_su\} \approx 0 \quad (r \neq s) \tag{38a,b,c}$$

we obtain:

$${}_sq_{0d}(j\omega) = -\frac{1}{{}_s\omega_0{}^2}\frac{1}{1-\left(\frac{\omega}{{}_s\omega_0}\right)^2 + j2{}_sh_0} \tag{39}$$

where:

$${}_s\omega_0{}^2 = \frac{\{{}_su\}^T[K]\{{}_su\}}{\{{}_su\}^T[M]\{{}_su\}}, \quad {}_sh_0 = \frac{1}{2}\frac{\{{}_su\}^T[K']\{{}_su\}}{\{{}_su\}^T[K]\{{}_su\}} \tag{40a,b}$$

and ${}_sh_0$ corresponds to the strain-energy proportional damping[18), 19)] of the s-th mode, as shown in Appendix 2.

Next, considering the case $\omega < 0$ in Eq. (4) and expressing the ratio of the solution $\{X(j\omega)\}$ to $X_g(j\omega)$ as a superposition of real eigenmodes $\{{}_su\}$, applying a similar procedure yields the following equation, which is the conjugate symmetric counterpart of Eq. (37).

$$\{\bar{G}_{0d}(j\omega)\} = \sum_{s=1}^{n} {}_s\beta\{{}_su\}\,{}_s\bar{q}_{0d}(j\omega) \tag{41}$$

where:

$${}_s\bar{q}_d(j\omega) = -\frac{1}{{}_s\omega_0{}^2}\frac{1}{1-\left(\frac{\omega}{{}_s\omega_0}\right)^2 - j2{}_sh_0} \tag{42}$$

The value of the transfer function $\{G_{0d}(0)\}$ at the singular point is given by Eq. (35). In a previous

study[18], which employed strain-energy proportional damping, seismic response calculations were conducted using a viscous damping system. This approach differs from the method presented in this chapter, which directly considers the complex damping system.

6. EXAMPLE OF NUMERICAL CALCULATION

Numerical calculations were performed using a building model (seismic vibration control structure) with the specifications shown in Table 1, as proposed in Ref. 17). This model is a six-degree-of-freedom shear-type system. In the original model, damping of approximately 13% is applied to the three lower floors equipped with dampers to achieve a first-mode damping ratio of around 10%. However, in this study, in order to more clearly observe the effects of non-proportional damping, a trial case with a larger damping ratio of 20% was considered.

Table 1 Building model

No.	m_i (ton)	k_i (kN/m)	h_i
6	200	60,000	0.02
5	200	70,000	0.02
4	200	75,000	0.02
3	200	80,000	0.20
2	200	85,000	0.20
1	200	95,000	0.20

The numerical calculations are conducted using three methods: the method based on simultaneous equations in Chap. 2 (hereinafter referred to as the direct method), the method based on the superposition of complex modes in Chap. 4 (the complex mode method), and the method based on the superposition of real modes in Chap. 5 (the real mode method).

Table 2 presents the natural frequencies and damping constants for each mode. The complex eigenvalue calculations are performed using the Stodola method[19] for complex problems. The norm error of the complex eigenvectors before and after iteration is set to be less than 10^{-7}. Here, ${}_sf(={}_s\omega/2\pi)$ represents the eigenfrequency obtained from the complex eigenvalue analysis, while ${}_sf_0(={}_s\omega_0/2\pi)$ is the eigenfrequency obtained from the real eigenvalue analysis. From Table 2, it can be observed that, in this case study, the damping ratio of the first mode is approximately 15%, and that the modal damping values ${}_sh_0$ obtained by the real mode method agree closely with those obtained by the complex mode method ${}_sh$ up to the fourth mode.

Table 2 Natural frequencies and damping

Mode No.	1	2	3	4	5	6
${}_sf$ (Hz)	0.793	2.21	3.57	4.57	5.51	6.02
${}_sf_0$ (Hz)	0.782	2.20	3.48	4.58	5.45	6.12
${}_sh$	0.147	0.077	0.088	0.102	0.051	0.180
${}_sh_0$	0.152	0.081	0.098	0.097	0.078	0.154

Figures 2(a)–(c) display the transfer functions of displacement, velocity, and acceleration of the top mass, respectively, comparing the results obtained by the direct method and the complex mode method. The upper panels of the figures show the response factor for an input of 1 gal ($= cm/s^2$), while the lower panels illustrate the phase characteristics. Both the response factor and phase characteristics exhibit perfect agreement between the direct method and the complex mode method, confirming the validity of the complex mode method.

Figure 3 compares the transfer functions obtained by the complex mode method and the real mode method. The differences between the two methods are minor in both response factors and phase characteristics.

Seismic response calculations are performed using the inverse Fourier transform[16] of the product of the Fourier transform of the input ground motion and the transfer function. The ground motion is the

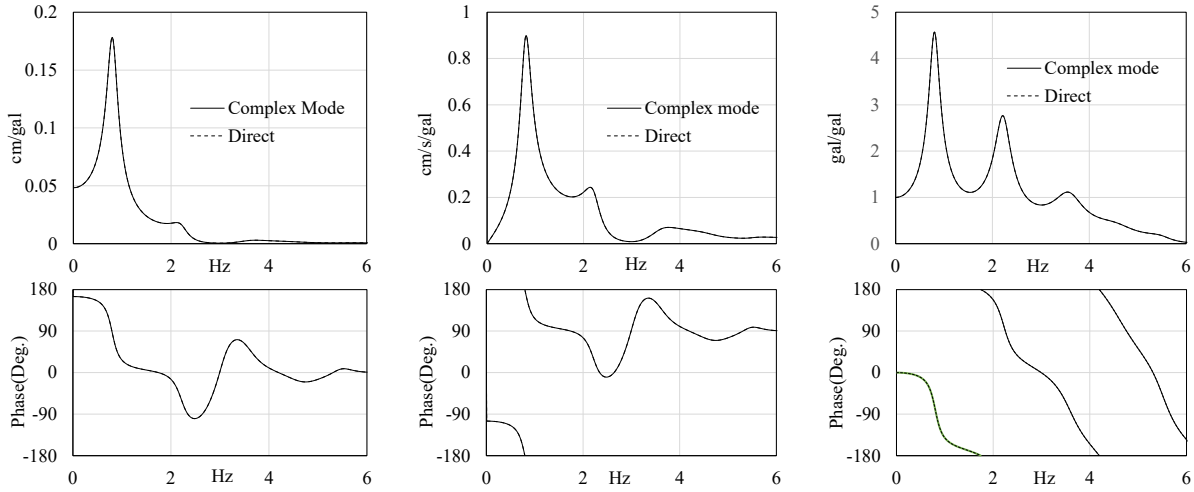

(a) Displacement (b) Velocity (c) Acceleration

Fig. 2 Transfer function (complex mode method vs. direct method)

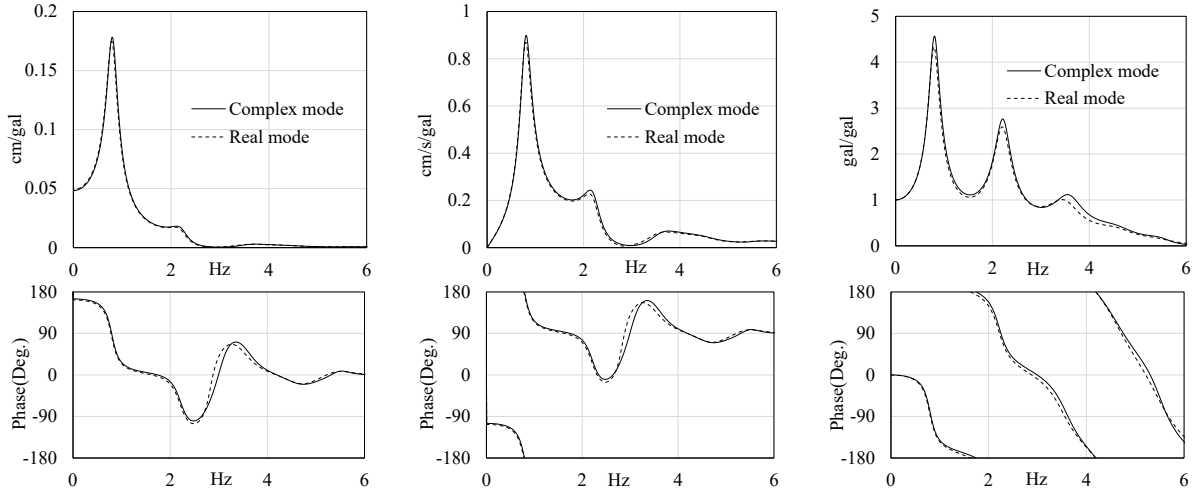

(a) Displacement (b) Velocity (c) Acceleration

Fig. 3 Transfer function (complex mode method vs. real mode method)

BCJ-L2 wave[20] with a maximum amplitude of 355 gal. The data length was set to 163.84 s by appending trailing zeros to the original 120 s wave, where 163.84 s corresponds to a time interval of 0.01 s multiplied by a total of 2^{14}. The total number of data points is set as a power of 2 to accommodate the fast Fourier transform method.

Figure 4 compares the maximum response values obtained by the complex mode method with those obtained by the real mode method. As expected from Fig. 3, the two methods show close agreement, demonstrating that the real mode method is a useful engineering approach. The maximum errors are 3% for displacement, 5% for velocity, and 8% for acceleration.

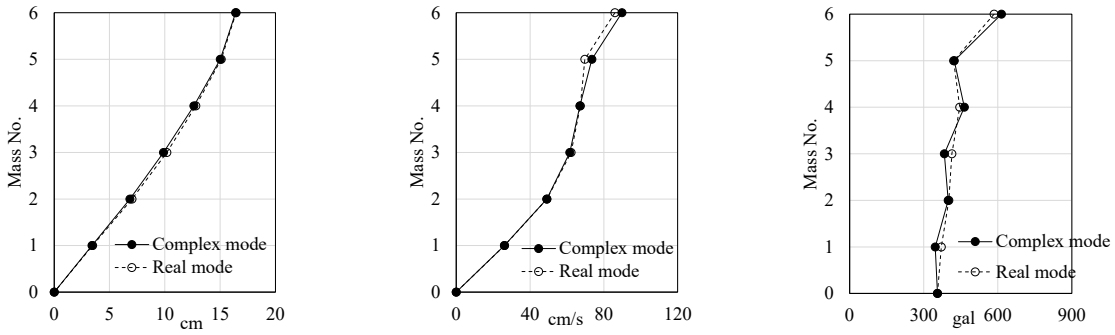

(a) Displacement (b) Velocity (c) Acceleration

Fig. 4 Maximum responses (complex mode method vs. real mode method)

7. CONCLUSIONS

(1) A method was presented for obtaining the complex eigenvalues and complex eigenvectors of forward and backward waves by solving the eigenvalue problem of the time domain equations of motion of a multi-mass model with non-proportional complex damping. This includes the damping force by Inaudi et al., expressed as the product of the Hilbert transform of the response displacement and the imaginary part of the complex stiffness. The application of the Hilbert transform utilizes the fact that free vibration consists of a single frequency component.

(2) Using the orthogonality of complex eigenvectors, it was shown that the transfer function of each mass can be represented as a superposition of the transfer functions of each mode, enabling complex modal analysis. Additionally, since the transfer function satisfies conjugate symmetry, it can be computed if the complex eigenvalues and complex eigenvectors of the forward wave for the system are known.

(3) Using real eigenvectors, the transfer function of each mass is expressed as a superposition of the transfer functions for each mode. Assuming approximate orthogonality of the damping matrix (the imaginary part of the complex stiffness), the obtained transfer function is also approximate. The modal damping in this model corresponds to energy-proportional damping.

(4) Numerical calculations were performed for a six-story vibration control structure with 20% damping in the bottom three stories. The calculations were conducted using the direct method (Chap. 2), the complex mode method (Chap. 4), and the real mode method (Chap. 5).

(5) A comparison of the transfer functions computed by the direct method and the complex mode method showed perfect agreement in both response factor and phase characteristics, verifying the validity of the complex mode method. A comparison between the complex mode method and the real mode method demonstrated that the response factor and phase characteristics were nearly identical.

(6) Seismic response calculations were conducted using the BCJ-L2 wave as input ground motion, employing both the complex mode and real mode transfer functions. The errors in the real mode method relative to the complex mode method for maximum response values were 3%, 5%, and 8%

for displacement, velocity, and acceleration, respectively, confirming that the real mode method is useful for engineering applications.

(7) The numerical model in this study assumed 20% damping in the lower three stories. The accuracy of the real mode method is influenced by the damping distribution and the input ground motion used, necessitating further investigation under different conditions. Future research should focus on the applicability of arbitrarily placed damping in vibration control structures and seismic isolation structures with significant damping at the base.

EXPLANATORY NOTE

This paper is a revised version of an abstract[21] submitted to the 17th Annual Conference of the Japan Association for Earthquake Engineering. Notably, in this paper, the symbol for the transfer function in the complex modal method has been changed from $\{G'_d(\mathrm{i}\omega)\}$ to $\{G_d(\mathrm{i}\omega)\}\}$. Additionally, the transfer function related to causality in the same abstract and Ref. 10) was found to correspond to the transfer function of the equivalent viscous damping model[6), 22)]. Consequently, the related descriptions have been omitted. The influence of non-causality remains a topic for future research.

APPENDIX 1: DERIVATION OF THE NATURAL CIRCULAR FREQUENCY—SUMMARY OF THE METHOD IN REFERENCE 10)

The eigenvalues for the case Re ω* > 0 are given by Eq. (16a), which is restated in Eq. (A1):

$$ {}_s\omega^{*2} = {}_s\omega^2(1 + j2\,{}_sh) \tag{A1} $$

Expressing the right-hand side of Eq. (A1) using Euler's relation:

$$ {}_s\omega^{*2} = \sqrt{1 + 4\,{}_sh^2}\ {}_s\omega^2 e^{j2\varphi} \tag{A2} $$

where

$$ \cos 2\varphi = \frac{1}{\sqrt{1 + 4\,{}_sh^2}},\quad \sin 2\varphi = \frac{2\,{}_sh}{\sqrt{1 + 4\,{}_sh^2}} \tag{A3a, b} $$

Using the double-angle formula, we obtain:

$$ \cos\varphi = \frac{\sqrt{1 + 4\,{}_sh^2} + 1}{\sqrt{\left(\sqrt{1 + 4\,{}_sh^2} + 1\right)^2 + 4\,{}_sh^2}},\quad \sin\varphi = \frac{2\,{}_sh}{\sqrt{\left(\sqrt{1 + 4\,{}_sh^2} + 1\right)^2 + 4\,{}_sh^2}} \tag{A4a, b} $$

Taking the square root of Eq. (A2):

$$ {}_s\omega^* = \pm\sqrt[4]{1 + 4\,{}_sh^2}\ {}_s\omega\ e^{j\varphi} = \pm\sqrt[4]{1 + 4\,{}_sh^2}\ {}_s\omega\ (\cos\varphi + j\sin\varphi) \tag{A5} $$

Substituting Eq. (A4) into the rightmost side of Eq. (A5) and rearranging:

$$ {}_s\omega^* = \pm\left(\sqrt{1 + {}_sh_e{}^2}\,{}_s\omega\ + j\,{}_sh_e\,{}_s\omega\right),\quad {}_sh_e = \sqrt{\frac{\sqrt{1 + 4\,{}_sh^2} - 1}{2}} \tag{A6a, b} $$

Here, the natural circular frequency ${}_s\omega^*$ of the forward wave satisfying Re ω* > 0 is again expressed in terms of ${}_s\omega_1^*$, yielding the following Eq. (A7), which corresponds to Eq. (17a) in the main text:

$$ {}_s\omega_1^* = \sqrt{1 + {}_s{h_e}^2}\,{}_s\omega \; + j\,{}_s h_e\,{}_s\omega \qquad (A7) $$

The case Re ω* > 0 has been discussed above, but a similar operation on Eq. (20) for the case Re ω* < 0 can be performed to obtain Eq. (21).

Although equations similar to Eq. (A6) can be found in Refs. 4) and 5), they are derived from inconsistent equations of motion and therefore lack logical coherence both in the derivation process and in the selection of eigenvalues.

APPENDIX 2: STRAIN ENERGY PROPORTIONAL DAMPING

Equation (40b) is restated as Eq. (A8), and it is shown that this equation is equivalent to the strain energy proportional damping model:

$$ {}_s h_0 = \frac{1}{2}\frac{\{{}_s u\}^T [K']\{{}_s u\}}{\{{}_s u\}^T [K]\{{}_s u\}} \qquad (A8) $$

The matrices $[K]$, $[K']$, and the vector $\{{}_s\Delta\}$ are expressed using the transformation matrix $[T]$ as follows:

$$ [K] = [T]^T \left[\ddots k_i \ddots\right][T], \quad [K'] = [T]^T \left[\ddots k_i' \ddots\right][T], \quad \{{}_s\Delta\} = [T]\{{}_s u\} \qquad (A9a, b, c) $$

here, $\{{}_s\Delta\}$ is a column vector whose elements represent the relative displacements ${}_s\Delta_i$ between the i-th and $(i-1)$-th masses in the s-th mode. In addition, [T] can be shown, using a three-mass system model as an example, as follows:

$$ [T] = \begin{bmatrix} 1 & 0 & 0 \\ -1 & 1 & 0 \\ 0 & -1 & 1 \end{bmatrix} \qquad (A10) $$

By substituting Eq. (A9) into Eq. (A8), the denominator and numerator can be rewritten as:

$$ 2\{{}_s u\}^T [K]\{{}_s u\} = 2\{{}_s u\}^T [T]^T \left[\ddots k_i \ddots\right][T]\{{}_s u\} = 2\{{}_s\Delta\}^T \left[\ddots k_i \ddots\right]\{{}_s\Delta\} = 2\sum_{i=1}^{n} k_i\,{}_s\Delta_i^2 = 4\sum_{i=1}^{n} {}_s E_i \qquad (A11a) $$

$$ \{{}_s u\}^T [K']\{{}_s u\} = \{{}_s u\}^T [T]^T \left[\ddots k_i' \ddots\right][T]\{{}_s u\} = \{{}_s\Delta\}^T \left[\ddots k_i' \ddots\right]\{{}_s\Delta\} = \sum_{i=1}^{n} k_i'\,{}_s\Delta_i^2 = 4\sum_{i=1}^{n} h_i\,{}_s E_i \qquad (A11b) $$

Here, ${}_s E_i$ represents the strain energy of the i-th element in the s-th mode, defined as:

$$ {}_s E_i = \frac{k_i\,{}_s\Delta_i^2}{2} \qquad (A12) $$

Substituting Eq. (A11) into Eq. (A8) yields:

$$ {}_s h_0 = \frac{\sum_{i=1}^{n} h_i\,{}_s E_i}{\sum_{i=1}^{n} {}_s E_i} \qquad (A13) $$

Equation (A13) is the fundamental definition of strain energy proportional damping[18].

REFERENCES

1) Satake, N., Arakawa, T. and Sasaki, A.: 5.2 Building Damping, *Damping in Buildings*, Architectural Institute of Japan, p. 134, pp. 138–139, 2000 (in Japanese).
2) Yasui, Y., Maeda, T. and Iguchi, M.: Estimation of Story Parameters from Microtremor Records Using Modal Responses of Substructures, *Proceedings of the 17th World Conference on Earthquake Engineering*, Sendai, Japan, 2i-0128, pp. 1–12, 2020.
3) Theodorsen, T. and Garrick, I. E.: Mechanism of Flutter, A Theoretical and Experimental Investigation of the Flutter Problem, National Advisory Committee for Aeronautics, 685, 47 pp., 1940.
4) Soroka, W. W.: Note on the Relations Between Viscous and Structural Damping Coefficients, *Journal of the Aeronautical Sciences*, Vol. 16, pp. 409–410, p. 448, 1949.
5) Bishop, R. E. D.: The Treatment of Damping Forces in Vibration Theory, *Journal of Royal Aeronautical Society*, Vol. 59, pp. 738–742, 1955.
6) Crandall, S. H.: Dynamic Response of Systems with Structural Damping, Air Force Office of Scientific Research, AFOSR 1561, Massachusetts Institute of Technology, Contract No. 49(638)-564, 25 pp., 1961.
7) Takizawa, H.: A Note on the Mathematical Structure of Linear Dynamic Systems (Part 2), *Transactions of the Architectural Institute of Japan,* Vol. 301, pp. 1–8, 1981 (in Japanese).
8) Milne, H. K.: The Impulse Response Function of a Single Degree of Freedom System with Hysteretic Damping, *Journal of Sound and Vibration*, Vol. 100, No. 4, pp. 590–593, 1985.
9) Inaudi, J. A. and Kelly, J. M.: Linear Hysteretic Damping and the Hilbert Transform, *Journal of Engineering Mechanics*, American Society of Civil Engineers, Vol. 121, No. 5, pp. 626–632, 1995.
10) Yasui, Y., Maeda, T. and Iguchi, M.: Vibration Characteristics of Single-Degree-of-Freedom Structure with Complex Damping, *Journal of Structural Engineering*, Architectural Institute of Japan, Vol. 67B, pp. 581–587, 2021 (in Japanese).
11) Nozu, A.: Hilbert Transform, Commentaries on Earthquake Engineering, Port and Airport Research Institute (in Japanese). https://www.pari.go.jp/bsh/jbn-kzo/jbn-bsi/taisin/tutorial_jpn.html (last accessed on June 1, 2022)
12) Aki, K. and Richards, P. G.: *Quantitative Seismology*, 2nd ed., University Science Books, pp. 152–153, 2002.
13) Tsushima, Y. and Jido, J.: Analysis of Multi-Degree of Freedom Systems with Complex Stiffness and Its Applications, (Part 1): Mode Super-Position Method Applied to Multi-Degree of Freedom Systems, *Transactions of the Architectural Institute of Japan,* Vol. 220, pp. 9–18, p.68, 1974 (in Japanese).
14) Sun, P., Yang, H. and Deng, Y.: Complex Mode Superposition Method of Nonproportionally Damped Linear Systems with Hysteretic Damping, *Journal of Vibration and Control*, Vol. 27 (13–14), pp. 1453–1465, 2021.
15) Foss, K. A.: Coordinates Which Uncouple the Equations of Motion of Damped Linear Dynamic Systems, *Journal of Applied Mechanics*, American Society of Mechanical Engineers, Vol. 25, No. 3, pp. 361–364, 1958.
16) Ohsaki, Y.: *New Introduction to Spectral Analysis of Earthquake Motions*, 10th Printing, Kajima Institute Publishing Co. Ltd., pp. 60–63, pp. 126–129, pp. 266–269, 2011 (in Japanese, title translated by the authors).
17) Ishimaru, S.: *How to Cope with Earthquakes—an Invitation to Dynamic Design*, Kenchiku-Gijutsu Co. Ltd., pp. 75–76, 2008 (in Japanese, title translated by the authors).
18) Roesset, J. M., Whitman, R. V. and Dobry, R.: Modal Analysis for Structures with Foundation Interaction, *Journal of the Structural Division*, American Society of Civil Engineers, Vol. 99, No. ST3, pp. 399–416, 1973.
19) Shibata, A.: *Latest Seismic Structural Analysis*, Morikita Publishing Co. Ltd., 1st ed., 17th printing, pp. 88–90, pp. 94–96, 2000 (in Japanese, title translated by the authors).

20) The Building Center of Japan: Download of Seismic Waves (in Japanese, title translated by the authors). https://www.bcj.or.jp/download/wave/ (last accessed on June 2, 2024)
21) Yasui, Y., Maeda, T. and Iguchi, M.: On the Eigenvalue Problem of a Multi-Degree-of-Freedom System with Complex Damping and the Transfer Function, *Proceedings of the 17th Annual Conference of the Japan Association for Earthquake Engineering*, TS_20220005, pp. 1–10, 2022 (in Japanese).
22) Maia, N.: Reflections on the Hysteretic Damping Model, *Shock and Vibration*, Vol. 16, pp. 529–542, 2009.

(Original Japanese Paper Published: November, 2024)
(English Version Submitted: March 27, 2025)
(English Version Accepted: August 19, 2025)